Anal. Bioanal. Electrochem., Vol. 9, No. 7, 2017, 904-928

Analytical & Bioanalytical Electrochemistry

2017 by CEE
www.abechem.com

Full Paper

Synthesis and Characterization of New Benzimidazoles Derivatives of 8-hydroxyquinoline as a Corrosion Inhibitor for Mild Steel in 1.0 M Hydrochloric Acid Medium

Mohamed Rbaa,[1] Mouhsine Galai,[2] Mohamed El Faydy,[1] Younes El Kacimi,[2] Mohamed Ebn Touhami,[2] Abdelkader Zarrouk[3] and Brahim Lakhrissi[1,*]

[1]*Laboratory of Agro-Resources, Polymers and Process Engineering, Department of Chemistry, Faculty of Sciences, Ibn Tofail University, PO Box 133, 14000, Kenitra, Morocco*
[2]*Laboratory of Materials Engineering and Environment: Application and Modeling, Faculty of Sciences, Ibn Tofail University, PO Box 133, 14000, Kenitra, Morocco*
[3]*LC2AME-URAC 18, Faculty of Science, First Mohammed University, PO Box 717, 60 000, Oujda, Morocco*

*Corresponding Author, Tel.: +212 611174149
E-Mail: b.lakhrissi2012@gmail.com or lakhrissi.brahim@uit.ac.ma

Received: 4 August 2017 / Received in revised form: 19 September 2017 / Accepted: 9 October 2017 / Published online: 15 November 2017

Abstract- A new benzimidazoles derivatives of 8-hydroxyquinoline, namely 5-((4-chlorophenyl)-benzimidazol-1-yl)-methyl)-quinolin-8-ol (**Q-Cl**) and 5-((2-phenylbenzimidazol-1-yl)-methyl)-quinolin-8-ol (**Q-H**) have been synthesized and their chemical structure has been elucidated and confirmed using ^{1}H and ^{13}C NMR spectroscopy s ^{1}H and ^{13}C NMR spectroscopy. Their inhibitive action against the corrosion of mild steel in 1.0 M hydrochloric acid solution were investigated at different temperatures in the range from 298 to 328±2 K by a series of known techniques such *as* weight loss, polarization and electrochemical impedance spectroscopy (EIS). It was found that the studied compounds exhibit a very good performance as inhibitors for mild steel corrosion in 1.0 M HCl. Results show that the inhibition efficiency increases with decreasing temperature and increasing concentration of inhibitor's. It has been determined that the adsorption for the studied inhibitors on mild steel complies with the Langmuir adsorption isotherm at all studied

temperatures. Results show that the order of inhibition efficiency is **Q-Cl** > **Q-H** due to the presence of electron donating -Cl group in **Q-Cl** thereby enhances its ability to donate charges to the metal during the adsorption process. The kinetic and thermodynamic parameters for mild steel corrosion and inhibitor's adsorption were determined and discussed. Scanning electron microscopy (SEM) confirmed both of the inhibitors played a significant protective effect in mild steel corrosion in 1.0 M HCl.

Keywords- Organic synthesis, NMR spectropscopy, Benzimidazole, Quinolin-8-ol, Mild steel, Corrosion, Inhibition,weight loss, EIS, SEM

1. INTRODUCTION

Iron and its alloys used in industrial sectors as building materials have become a major challenge for corrosion engineers or scientists [1], So, in order to remove the scale and other products from the metal working, cleaning of boilers and heat exchangers, the acid solutions are commonly used. In these cases the metals were damaged by corrosion phenomena. Thus, to minimize this problem, many inhibitors are used [2]. In addition, organic compounds have many advantages such as high inhibition efficiency [3], low price, and easy production. Today, the development of new corrosion inhibitors based on organic compounds having multiple bonds, nitrogen and/or sulfur atoms in their structures have been employed. Among these, several triazoles [4,5], tetrazole [6], phenyltetrazole [3,7], imidazoles [8,9], quinoxaline [10], quinolinol [11], quinoline [12-15], have been used as corrosion inhibitors for metals in corrosive medium. In literature review and for the specific case of the derivatives of 8-hydroxyquinoline are shown to be a good corrosion inhibitor of ordinary steel in acidic media [12-15]. Furthermore, 8-aminoquinoline compounds have been applied as chemotherapeutic agents for the treatment of malaria disease [16]. Also, many quinolines and their derivatives have biological activities such as DNA binding capacities [17], anti-tumor [18], DNA-interleaving transporter [19] and antibacterial [20].

As a follow-up to our previous work, we present in this study the effect of the substitution of the hydrogen atom (-H) by the chlorine atom (-Cl) on the corrosion inhibiting properties of 2-(substituted phenyl)-benzimidazole derivatives on mild steel in 1 M HCl solution. For that, the synthesis and characterization of two benzimidazoles derivatives of 8-hydroxyquinoline, namely 5-((2-phenylbenzimidazol-1-yl)-methyl)-quinolin-8-ol (**Q-H**) and 5-((4-chlorophen-yl)-benzimidazol-1-yl)-methyl)-quinolin-8-ol (**Q-Cl**) have been carried out and their corrosion inhibition properties on mild steel in 1.0 M HCl were studied. The adsorption and inhibition efficiency of these inhibitors were investigated using weight loss, electrochemical impedance spectroscopic (EIS) and potentiodynamic polarization methods (Tafel) and the thermodynamic adsorption parameters were calculated. The effect of temperature on the corrosion behavior was also studied in the range from 298 to 328±2 K. Scanning Electron Microscopy (SEM) was performed and discussed for surface study of uninhibited and inhibited mild steel samples.

2. MATERIALS AND METHODS

2.1. Description of materials and products

Unless otherwise stated, all the reagents and solvents used in this study were obtained from Sigma-Aldrich Chemical Company (Spain or France). Melting points were determined on Banc Kofler apparatus and are uncorrected. The recording of NMR spectra was performed on a Bruker Advanced 300 WB at 300 MHz for solutions in Me_2SO-d_6 and chemical shifts are given in δ_{ppm} with reference to tetramethylsilane (TMS) as an internal standard. The progress of the reaction is followed by chromatography with thin layer (TLC) of silica 60 F254 (E. Merck).

The chemical composition of steel is shown in Table 1. The specimen's surface was prepared by polishing with emery paper at different grit sizes (from 180 to 1200), rinsing with distilled water, degreasing in ethanol, and drying at hot air.

Corrosion tests were performed on mild steel which had the following chemical composition *(wt %)* balanced with (Fe).

Table 1. Chemical composition of carbon steel

Composition	C	Si	P	Al	Mn	S	Fe
wt %	0.21	0.38	0.38	0.38	0.05	0.05	Balance

The aggressive solution of 1.0 M HCl was prepared by dilution of analytical grade 37% HCl with distilled water.

2.2. Synthesis of 8-hydroxyquinolines derivatives of benzimidazole (Q-H and Q-Cl)

The synthesis of 5-((2-phenylbenzimidazol-1-yl)-methyl)-quinolin-8-ol **(Q-H)** and 5-((2-(4-chlorophenyl)-benzimidazol-1-yl)-methyl)-quinolin-8-ol **(Q-Cl)** is produced by condensation of 5-chloromethyl-8-hydroxyquinoline hydrochloride **2** with 2-alkylbenzimidazoles (**5a,b**) in the presence of potassium carbonate in dimethylformamide at 80 °C for 16 h (scheme 1).

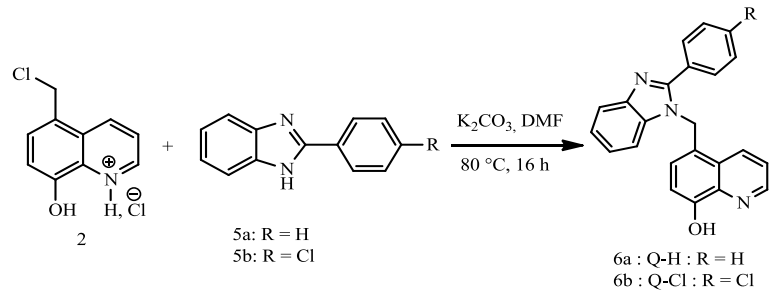

Scheme 1. Synthetic route for the preparation of compounds **Q-H** and **Q-Cl**

2.2.1. Synthesis of 5-chloromethyl-8-hydroxyquinoline hydrochloride (2)

The 5-chloromethyl-8-hydroxyquinoline hydrochloride (**2)** was prepared by adopting the method of Feng et al. [21], which consists of a treatment of the mixture of 8-hydroxyquinoline **1**, formaldehyde (40%) and concentrated hydrochloric acid (37%) with dry hydrogen chloride gas at route temperature for 24 h (scheme 2).

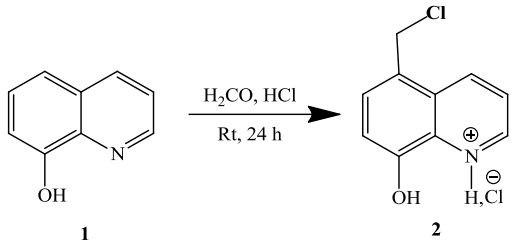

Scheme 2. Synthetic route for the preparation of 5-chloromethyl-8-hydroxyquinoline hydrochloride **2**

2.2.2. Synthesis of 2-phenylalkylbezimidazoles 5a,b

The synthesis of 2-phenylbenzimidazole **5a** and 2-(4-chlorophenyl)-benzimidazole **5b** was realized according to the method described by Fortenberry et al. [22], which consists in the condensation of *o*-phenylenediamine **3** with the substituted benzaldehydes **4a,b** in the presence of ammonium hydrochloride in absolute ethanol at room temperature for 24 h (scheme 3).

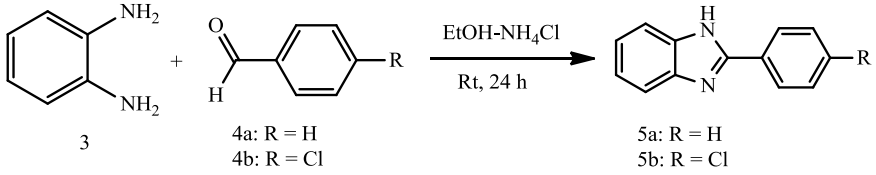

Scheme 3. Synthetic route for the preparation of 2-phenylalkylbezimidazoles **5a,b**

2.2.3. General procedure for the synthesis of 5-((2-phenylbenzimidazol-1-yl)-methyl)-quinolin-8-ol (Q-H) and 5-((2-(4-chlorophenyl)-benzimidazol-1-yl)-methyl)-quinolin-8-ol (Q-Cl)

A mixture of 2-alkylbenzimidazoles (0.01.0 mol) of 5-chloromethyl-8-hydroxyquinoline hydrochloride (0.02 mol) in the presence of K_2CO_3 (0.02 mol) in dimethylformamide (45 mL) is heated at 80 °C, with magnetic stirring for 24 h. The reaction was followed by TLC, after cooling; the reaction mixture was added to 20 ml of water and then extracted with chloroform (3×20 mL). The organic layers are combined, washed with saturated

aqueous sodium chloride (otherwise known as brine), dried over anhydrous magnesium sulfate and concentrated to dryness on a rotary evaporator. The obtained crude product was recrystallized from absolute alcohol.

The yields and physicochemical characteristics are summarized in Table 2.

Table 2. Yields and physicochemical properties of the synthesized compounds

Product	Yield (%)	Mp (°C)	Spectral data
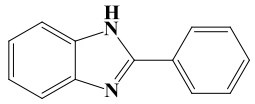 *5a*	98	>260	^{1}H NMR (300 MHz, DMSO-d_6), δ: 12.93 (s, 1H, NH), 7.17-8.18 (m, 9H, ArH). ^{13}C NMR (300 MHz, DMSO-d6): δ: 151.7 ((N=C(ph)N), 135.5-144.3 (Ar-C benzene ring of imidazole) 111.8-123.0-126.9-129.4-130.6 (Ar-CH of benzene ring).
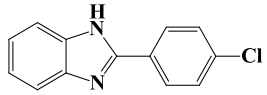 *5b*	97	>260	^{1}H NMR (300 MHz, DMSO-d_6), δ: 12.99 (s, 1H, NH), 7.19-8.18 (m, 8H, ArH). ^{13}C NMR (300 MHz, DMSO-d_6), δ: 150.6 ((N=C(ph)N), 135.0 (Ar-C-Cl) 131.2-129.5 (Ar-C benzene ring of imidazole), 111.9-123.3-128.8-129.3 (Ar-CH of benzene ring).
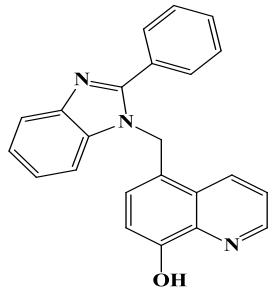 **Q-H**	79	186	^{1}H NMR (300 MHz, DMSO-d_6), δ: 5.12 (s, 1H, OH), 6.14 (s, 2H, CH_2), 7.36-7.54-7.61-7.62-8.46 (m, 9H, Aromatic of benzimidazole), 7.04-7.60-7.63-8.49-8.874 (m, 5H, Aromatic of quinoline). ^{13}C NMR (300 MHz, DMSO-d_6), δ: 51.43 (CH_2), 152.68 (Ar-C-OH), 154.46 ((N=C(ph)N), 124.50-121.82 (Ar-CH benzene ring of imidazole), 139.29- 136.25- (Ar-C benzene ring of imidazole), 129.24-127.62-133.11 (Ar-CH of benzene ring), 129.10 (Ar-C of benzene ring), 148.12-127.62-129.08-121.82-110.86 (Ar-CH of quinoline), 136.39-128.56-126.40 (Ar-C of quinoline).
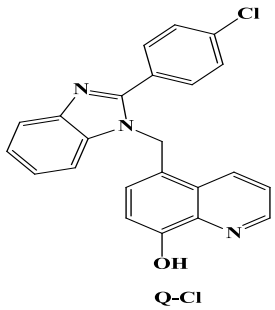 **Q-Cl**	75	135	^{1}H NMR (300 MHz, DMSO-d_6), δ: 5.06 (s, 1H, OH), 5.72 (s, 2H, CH_2), 7.40-7.58-7.59-8.46 (m, 8H, Aromatic of benzimidazole), 7.03-7.56-7.60-8.49-8.86 (m, 5H, Aromatic of quinoline). ^{13}C NMR (300 MHz, DMSO-d_6), δ: 69.53 (CH_2), 152.35 (Ar-C-OH), 153.91 ((N=C(ph)N), 119.69-124.63 (Ar-CH benzene ring of imidazole), 133.57-139.31 (Ar-C benzene ring of imidazole), 128.52-129.26 (Ar-CH of benzene ring), 128.27-133.57 (Ar-C of benzene ring), 132.69-148.76-126.99-122.15-111.16 (ArCH of quinoline), 139.17-127.74-124.63 (Ar-C of quinoline).

2.3. Weight loss measurements

Weight loss experiments were done according to ASTM methods described previously [23]. Tests were conducted in 1.0 M of HCl for 6 h at 298±K. Gravimetric measurements were carried out in an electrolysis cell equipped with a thermostat-cooling condenser. The mild steel specimens used have a rectangular form 2.5 cm×2.0 cm×0.05 cm. After immersion period, the specimens were cleaned according to ASTM G-81 and reweighed to 10^{-4} g for determining corrosion rate [24]. Duplicate experiments are performed in each case, and the mean value of the weight loss is reported. Weight loss allows us to calculate the mean corrosion rate as expressed in ($mgcm^{-2}h^{-1}$), either by chemical analysis of dissolved metal in solution or by gravimetric method measuring. The corrosion rate (ω_{corr}) is thereby the fundamental measurement in corrosion, it can be determined by weighing the cleaned samples before and after hanging the specimens into the aggressive solution by applying the following equation (1):

$$\omega_{corr} = \frac{m_i - m_f}{S \times t} \quad (1)$$

where m_i, m_f, S and t denote initial weight, final weight, surface of specimen and immersion time, respectively.

The value of the inhibiting efficiency was calculated by the following equation (2):

$$\eta_{\omega}(\%) = \frac{\omega^{0}_{corr} - \omega_{corr}}{\omega^{0}_{corr}} \times 100 \quad (2)$$

Where ω°_{corr} and ω_{corr} are the corrosion rates in the absence and presence of inhibitors, respectively.

2.4. Electrochemical cell

For electrochemical measurements, the electrolysis cell closed by a cap with five apertures. The working electrode was pressure-fitted into a polytetrafluoroethylene holder (PTFE) exposing only 1 cm^2 of area to the aggressive solution. Pt and saturated calomel were used as counter and reference electrode (SCE), respectively. All potentials were measured against the last electrode.

The potentiodynamic polarization curves were recorded by changing the electrode potential automatically from negative values to positive values versus E_{corr} using a Potentiostat/Galvanostat type PGZ 100, with a scan rate of 1 mV/s after 1 h of immersion time unti reaching steady state. The test solution was thermostatically controlled at 298±1 K in air atmosphere without bubbling. To evaluate corrosion kinetic parameters, a fitting by Stern-Geary equation was used [25]. The corrosion inhibition efficiency was evaluated from the corrosion current densities values using the relationship (3):

$$\eta_{PP} = \frac{i^{0}_{corr} - i_{corr}}{i^{0}_{corr}} \times 100 \quad (3)$$

The surface coverage values (θ) have been obtained from polarization curves for various concentrations of inhibitor using the following equation (4):

$$\theta = 1 - \frac{i_{corr}}{i^{0}_{corr}} \quad (4)$$

Where i^{0}_{corr} and i_{corr} are the corrosion current densities values without and with inhibitor, respectively.

Finally, the electrochemical impedance spectroscopy measurements were carried out using a Transfer Function Analyzer, with a small amplitude a.c. signal (10 mV rms), over a frequency domain from 100 kHz to 100 mHz with five points per decade. The results were then analyzed in terms of an equivalent electrical circuit using EC-Lab software. The inhibition efficiencies η_{EIS} %, were calculated from Nyquist plots by the equation (5):

$$\eta_{EIS}(\%) = \left(\frac{R_{ct} - R^{\circ}_{ct}}{R_{ct}} \right) \times 100 \quad (5)$$

Where R°_{ct} and R_{ct} are the charge transfer resistance of steel electrode in absence and in presence of inhibitor.

In order to ensure producibility, all experiments were repeated three times where the evaluated inaccuracy did not exceed 10%.

3. RESULTS AND DISCUSSION

3.1. Comparative study with previous work (Weight loss studies)

Many researchers studied corrosion inhibition by numerous quinoline derivatives. It is demonstrated that the quinoline compounds are good inhibitor's for metals corrosion in different solution [12-15]. Table 3 reports the type and corrosion mechanism inhibition for some selected quinoline derivatives used as corrosion inhibitors in HCl medium. Since there is no general explanation for the effect of substitution on corrosion inhibition properties of 8-hydroxyquinoline derivatives on mild steel in 1.0 M HCl solution. For that, we have reported in a recent study the effect of the substitution of (-NO_2) by (-N(CH_3)) on the aromatic nucleus of 8-hydroxyquinoline on its corrosion inhibiting properties of mild steel in a 1.0 M HCl solution [12]. The experimental results showed that the corrosion inhibition depended on the substitution on the aromatic nucleus of 8-hydroxyquinoline. In the following and in continuation of our previous work, we present in this study the effect of the substitution of

hydrogen atom (-H) by chlorine atom (-Cl) on the corrosion inhibition properties of 2-(substituted phenyl)-benzimidazole derivatives on mild steel in 1.0 M HCl solution.

Table 3. Adsorption isotherme and inhibitor type for different quinoline derivatives used as corrosion inhibitors for steels in acidic medium

N°	Compounds	Materials	Mild	[C] (M)	Adsorption isotherm	Inhibitor type	Ref.
1	5-((2-(4-dimethylamino)-phenyl-1H-benzo[d]imidazol-1-yl)-methyl)-quinolin-8-ol	Mild steel	1.0 M HCl	10^{-6} to 10^{-3}	Langmuir	Mixed type	[12]
2	5-((2-(4-nitrophenyl)-1H-benzo[d]imidazol-1-yl)-methyl)-quinolin-8-ol	Mild steel	1.0 M HCl	10^{-6} to 10^{-3}	Langmuir & Thermodynamic-kinetic model of El-Awady	Mixed type	[12]
3	8-hydroxyquinoline	Cold rolled steel	0.5 M H_2SO_4	10^{-3} to 1.2 10^{-3}	Temkin	Mixed type	[13]
4	8-hydroxyquinoline/sodium chloride (NaCl)	Cold rolled steel	0.5 M H_2SO_4	10^{-3} to 1.2 10^{-3}	Langmuir	Mixed type	[13]
5	Quinoline	Mild steel	3.0 M HCl	10^{-4} to 10^{-2}	Langmuir	Mixed type	[14]
6	8-hydroxyquinoline	Mild steel	3.0 M HCl	10^{-4} to 10^{-2}	Langmuir	Mixed type	[14]
7	Quinoline-2-thio	Mild steel	3.0 M HCl	10^{-4} to 10^{-2}	Langmuir	Mixed type	[14]
8	*N*-(8-hydroxyquinolin-5-yl)-methyl)-*N*-phenylacetamide	XC38 Steel	1.0 M HCl	10^{-6} to 10^{-3}	Langmuir	-	[15]

The corrosion rate values (ω_{corr}) of mild steel in 1.0 M HCl at different concentrations of substituted quinoline are presented in Table 4. It is noted that all substituted quinoline compounds act as good corrosion inhibitor's and their inhibition increase with their concentrations and follow the order: **Q-Cl** > **Q-N(CH_3)** > **Q-H** > **Q-NO_2**. This order can be explained by the rise of the effective electrondensity at the functional group of inhibitors [3].

Table 4. Weight loss data of mild steel 1.0 M HCl at various concentration of quinoline derivatives at 298 K

Inhibitor	**[C] (M)**	ω_{corr} **(mgcm^{-2}h^{-1})**	η_{ω} **(%)**	**θ**
Blank	00	37.22	—	—
Q-H	10^{-6}	9.44	74.70	0.747
	10^{-5}	7.79	79.10	0.791
	10^{-4}	5.53	85.20	0.852
	10^{-3}	4.01	89.00	0.890
Q-Cl	10^{-6}	8.33	77.60	0.776
	10^{-5}	6.03	83.70	0.837
	10^{-4}	4.98	86.60	0.866
	10^{-3}	2.79	92.50	0.925
Q-N(CH$_3$)$_2$ [12]	10^{-6}	9.20	76.4	0.764
	10^{-5}	6.01	84.6	0.846
	10^{-4}	3.89	90.1	0.901
	10^{-3}	2.67	93.1	0.931
Q-NO$_2$ [12]	10^{-6}	32.70	32.7	0.327
	10^{-5}	19.20	50.7	0.507
	10^{-4}	18.01	53.7	0.537
	10^{-3}	6.67	82.9	0.829

So, the compounds have aromatic or heterocyclic ring, the effective electron density at the functional group can be change by the introduction of different substituent's in the ring causing the variations on their molecular structure; therefore a change in their corrosion inhibition efficiencies. It is apparent also that an increase of η_{ω} (%) with inhibitor concentrations, reaching a maximum value at of 10^{-3} M for both inhibitor's, but better performances were obtained by **Q-N(CH$_3$)$_2$** is known to the presence of electron donating (–CH_3) group in **Q-N(CH$_3$)**. However, the best performance of newly synthesized compound (**Q-Cl**) as corrosion inhibitor over compounds **Q-NO$_2$** and **Q-H** may be attributed to the presence of (–Cl) group in compound **Q-Cl**. The nucleophilic (electron releasing) character of (–Cl) group is highest than the electrophonic (electron withdrawing). **Q-Cl** can produce protonated species in HCl by the reaction of the amino group with HCl. This ammonium substituent may reduce the electronic density on the substituted quinoline compounds. The same results were observed by El Kacimi et al. [3,7]. Maximum values of (inhibition efficiency) 93.1% for **Q-N(CH$_3$)** and 92.5% for **Q-Cl** were obtained at 10^{-3} M. These results

are comparable with those calculated from weight loss measurements in Table 2 but a little difference can be observed.

In order to confirm the best protective properties of newly 5-((2-phenylbenzimidazol-1-yl)-methyl)-quinolin-8-ol (**Q-H**) and 5-((4-chlorophenyl)-benzimidazol-1-yl)-methyl)-quinolin-8-ol (**Q-Cl**) in 1.0 M HCl medium, the effect of concentration and temperature, was investigated using ac and dc electrochemical techniques.

3.2. Potentiodynamic polarization studies

The potentiodynamic polarization behavior of mild steel in 1.0 M of HCl solution without and with different concentrations of all substituted quinoline compounds are shown in Figure 1 and Figure 2. Their electrochemical data are given in Table 5. It is known that the electrochemical reactions of the mild steel in acidic medium, in the absence of inhibitors, is the anodic dissolution reaction of iron and cathodic reactions related to the proton reduction:

$$Fe \leftrightarrow Fe^{2+} + 2e^- \quad (6)$$

$$2\,H^+ + 2e^- \leftrightarrow H_2 \quad (7)$$

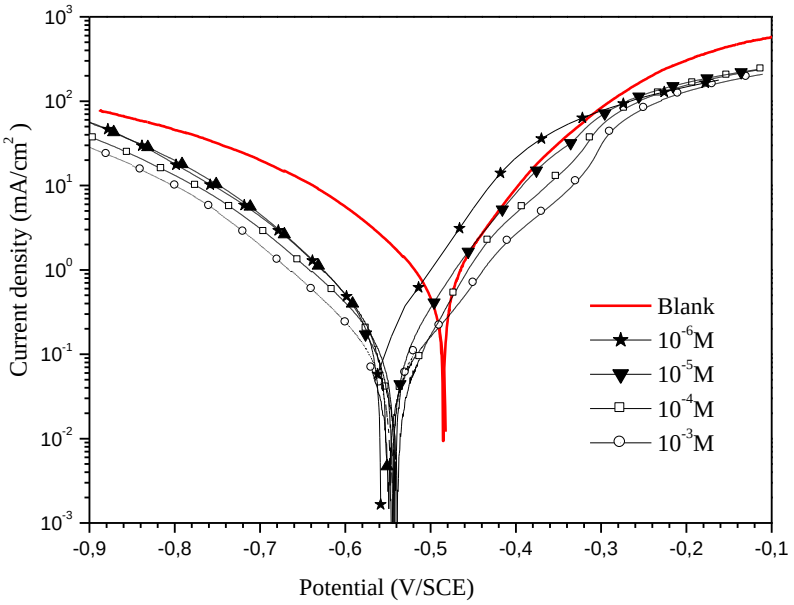

Fig. 1. Potentiodynamic polarization curves for mild steel in 1.0 M HCl at various concentration of **Q-H**

However, in the presence of inhibitors, a shift of the corrosion potential E_{corr} towards more negative values for all compounds was observed. So, a great definite change on the corrosion potential (E_{corr}) was observed. According to Riggs [26], if the displacement in E (i) is>85 mV/E_{corr}, the inhibitor can be seen as a cathodic or anodic type, (ii) if displacement in E

is<85 mV/E_{corr}, the inhibitor can be seen as mixed type. In our study, the displacement in the case of all products were lower than 85 mV/E_{corr}, indicated that **Q-H** and **Q-Cl** were effective mixed type inhibitors.

In addition, it is clear that the current density decreases with increasing of the substituted quinoline concentration; this indicates that these compounds are adsorbed on the metal surface and hence inhibition occurs.

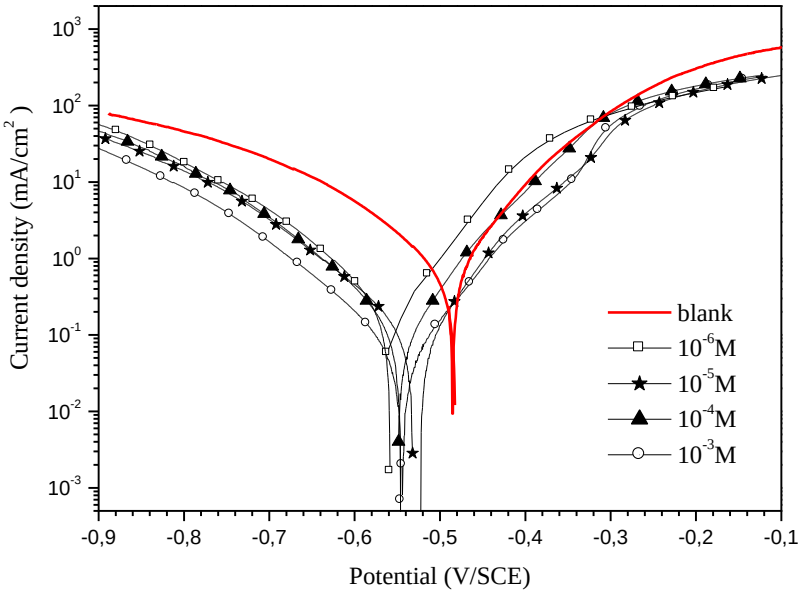

Fig. 2. Potentiodynamic polarization curves for mild steel in 1.0 M HCl at various concentration of **Q-Cl**

Table 5. Potentiodynamic electrochemical parameters obtained for mild steel in 1.0 M HCl at various concentrations of **Q-H** and **Q-Cl** at 298 K

Inhibitor	**[C] (M)**	**-E_{corr} (mV_{SCE})**	**-β_c ($mVdec^{-1}$)**	**i_{corr} (μAcm^{-2})**	**η_{pp} (%)**	**θ**
Blank	00	485.0	220.0	983	—	—
Q-H	10^{-6}	557.5	118.3	333	66.12	0.661
	10^{-5}	550.1	112.1	268	72.74	0.727
	10^{-4}	541.7	107.4	196	80.06	0.801
	10^{-3}	545.3	104.3	132	86.57	0.866
Q-Cl	10^{-6}	557.7	106.2	315	67.96	0.679
	10^{-5}	544.8	98.5	227	76.91	0.769
	10^{-4}	530.7	97.6	141	85.66	0.856
	10^{-3}	543.7	90.1	96	90.23	0.902

The potentiodynamic polarization curves (Figures 1 and 2) shows that these inhibitors have an effect on both, the cathodic and anodic slopes (β_c and β_a) and suppressed both cathodic and anodic processes. This indicated a modification of the mechanism of cathodic hydrogen evolution (equation (7)) as well as anodic dissolution of iron (equation (6)), which suggest that the substituted quinoline powerfully inhibit the corrosion process of mild steel, and their ability as corrosion inhibitors are enhanced as their concentrations are increased. The suppression of cathodic process can be due to the covering of the mild steel surface with monolayer due to the adsorbed inhibitor molecules. The corrosion inhibition efficiency is evaluated from the corrosion current densities values using the relationship (3). It is seen also that all compounds bring down (i_{corr}) value at all concentrations, the minimum values was obtained at 10^{-3} M and the η_{PP} followed the order: **Q-Cl** > **Q-H** such as found by the weight loss measurements.

3.3. Electrochemical impedance measurements

Figures 3 and 4 show typical Nyquist plots for the mild steel in 1.0 M HCl in absence and presence of different concentrations of **Q-H** and **Q-Cl**. All of the impedance spectra mainly display depressed semicircles.

The impedance response of mild steel in 1.0 M HCl solution was significantly changed after the addition of both inhibitors and the impedance of the inhibited system increased with inhibitor concentration. Furthermore, at 10^{-3} M concentration of **Q-H** and **Q-Cl** larger diameter semicircles were obtained than the other three lower concentrations of these compounds (Figures 3 and 4).

The impedance diagrams presented in the Nyquist plan are in the form of semicircles whose sizes increase with the inhibitor concentration, indicating a well-defined charge transfer process and improved protection in the presence of the studied organic inhibitors. However, it allowed employing CPE element in order to investigate the inhibitive film properties on metallic surface. Thus, the impedance of the CPE can be described by the following equation (8).

$$Z_{\mathrm{CPE}} = \left[Q(j\omega)^n \right]^{-1} \qquad (8)$$

With j is the imaginary number, Q is the frequency independent real constant, $\omega=2\pi f$ is the angular frequency (rad s^{-1}), $f$is the frequency of the applied signal, n is the CPE exponent for whole number of n=1, 0, -1, CPE is reduced to the classical lump element-capacitor (C), resistance (R) and inductance (L) [27]. The use of these parameters, similar to the constant phase element (CPE), allowed the depressed feature of Nyquist plot to be reproduced readily. In addition, the effective calculated double layer capacitance (C) derived from the CPE parameters [28] according to the following equation (9):

$$C = Q^{\frac{1}{n}} \times R^{\frac{(1-n)}{n}} \quad (9)$$

It is apparent that the obtained spectra were composed of one capacitive loop which its diameter was significantly increased after inhibitors addition to reach a maximum at 10^{-3} M. In addition, these diagrams are not perfect semicircles which have been attributed to frequency dispersion [29].

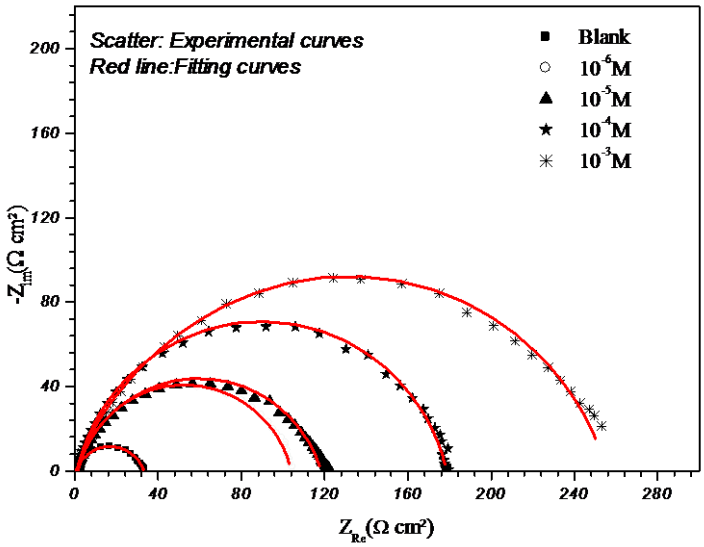

Fig. 3. Nyquist plots for mild steel in 1.0 M HCl at open circuit potential in the absence and presence of **Q-H** at various concentration: (scater) experimental; (red line) fitted data using structural model in Figure 6

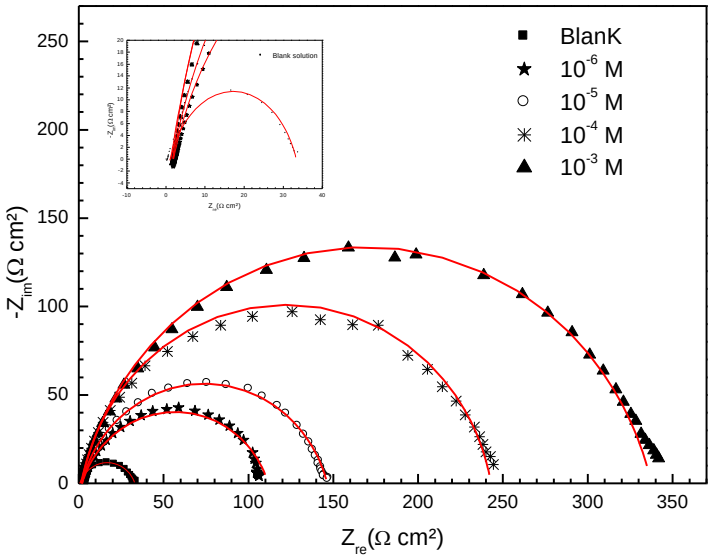

Fig. 4. Nyquist plots for mild steel in 1.0 M HCl at open circuit potential in the absence and presence of **Q-Cl** at various concentration: (scater) experimental; (red line) fitted data using structural model in Figure 6

However, the inhibitors addition is found to enhance R_{ct} values and bring down C_{dl} values. These finding can be explained by the fact that the mild steel corrosion in 1.0 M HCl was controlled by a charge transfer process and the corrosion inhibition occurs by the adsorption of the substituted quinolone compounds on mild steel surface. However, the decrease in the C_{dl} values, with can result from a decrease in local dielectric constant and/or an increase in courant density, the thickness of the electrical double layer, suggested by adsorption of the quinoline molecules at the metal/solution interface [31,32]. It is noted also that the inhibition efficiency follow the order: **Q-Cl** > **Q-H**, which is in a good agreement with results obtained from weight loss and potentiodynamic polarization measurements.

Figures 3 and 4 show only one depressed capacitive loop at the higher frequency range (HF) with one capacitive time constant in the Bode-phase plot. In this case, the standard Randles' circuit model of Figure 6 which has been previously used [32], fits well our experimental results. According to the above-mentioned equivalent circuits, the solution resistance R_s, the charge transfer resistance R_{ct} and the constant phase element (CPE) were fitted and their parameters were calculated according to this circuit and were listed in Table 6.

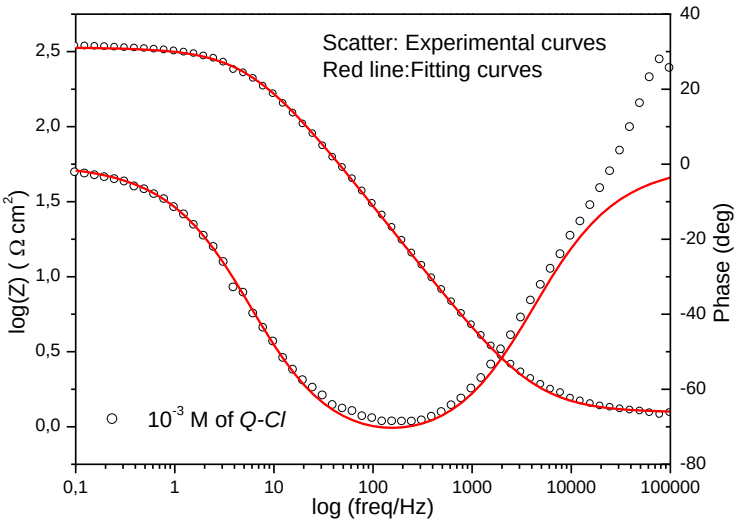

Fig. 5. Bode diagrams for mild steel/1.0 M HCl interface with 10^{-3} M of **Q-Cl**: (⋯) experimental; (—) fitted data using structural model in Figure 6

From the Nyquist diagrams, the model of the equivalent circuit explaining these experimental results is represented by Figure 6.

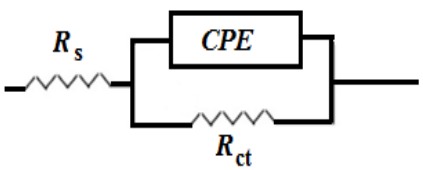

Fig. 6. Electrical equivalent circuit applied for impedance analysis

Table 6. Impedance data for mild steel in 1.0 M HCl at various concentration of **Q-Cl** and **Q-H** at 298 K

Inhibitor	[C] (M)	R_{ct} (Ωcm^2)	C_{dl} ($\mu F cm^{-2}$)	n_{dl}	η_{EIS} (%)
Blank	00	35.0	284.0	0.79	—
Q-H	10^{-6}	104.8	121.8	0.86	66.60
	10^{-5}	120.0	106.8	0.82	70.83
	10^{-4}	178.8	89.1	0.86	80.43
	10^{-3}	260.0	77.1	0.81	86.54
Q-Cl	10^{-6}	104.0	240.0	0.80	66.35
	10^{-5}	149.0	224.0	0.81	76.51
	10^{-4}	250.0	111.0	0.84	86.00
	10^{-3}	350.0	78.7	0.85	90.00

It is remarked also that the n_{dl} values increase with increasing of the inhibitors concentrations. This can be explained by the decrease in surface heterogeneity as a result of the quinoline molecules adsorption on the mild steel surface. The same result was found by other authors, and they explained by the molecule adsorption of inhibitors via *N* and *S* atoms in the inhibitor molecules [15].

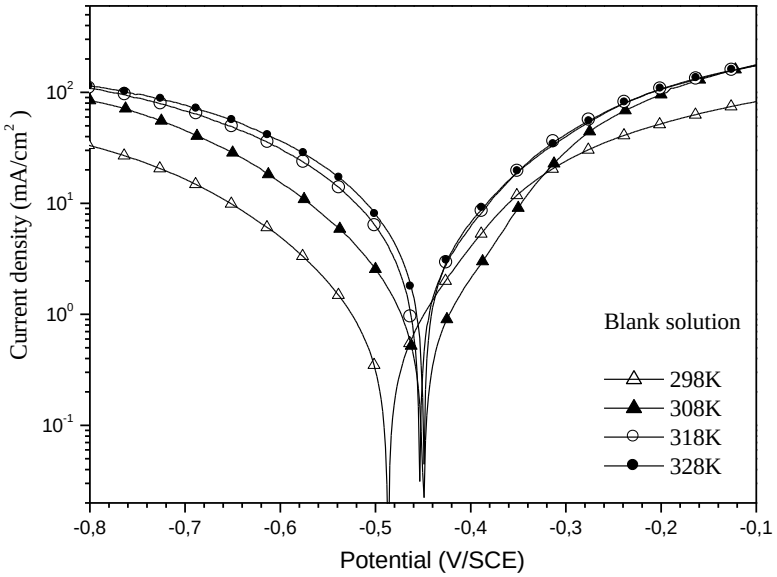

Fig. 7. Polarization curves at different temperatures for the behavior of mild steel in 1.0 M HCl without inhibitor

In the other hand, it is observed that the electrolyte solution increased with the inhibitors addition. This can be explained by the protonation of the inhibitor molecules decreasing therefore the concentration of the H^+ ions in the solution. It is noted also that the inhibition efficiency follow the order: **Q-C l** > **Q-H**, which is in a good agreement with results obtained from weight loss and potentiodynamic polarization measurements.

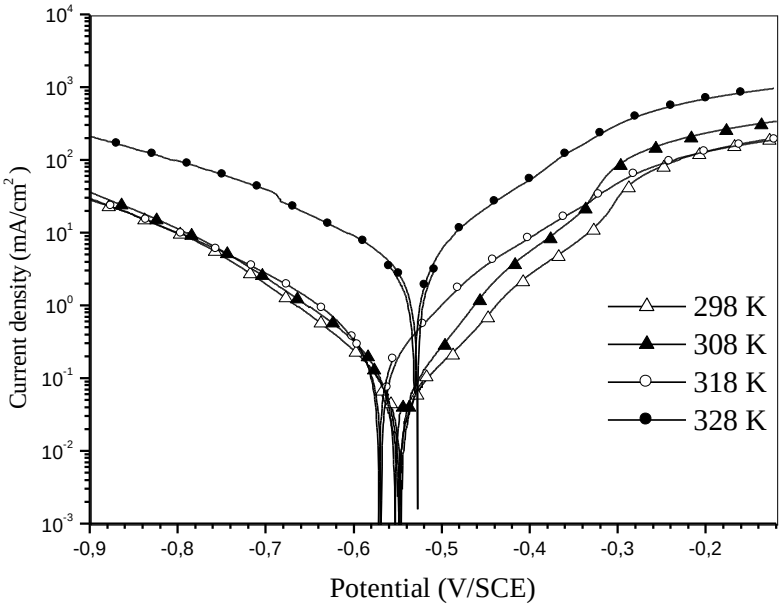

Fig. 8. Potentiodynamic polarization curves of mild steel in 1.0 M HCl at various concentration of **Q-H**

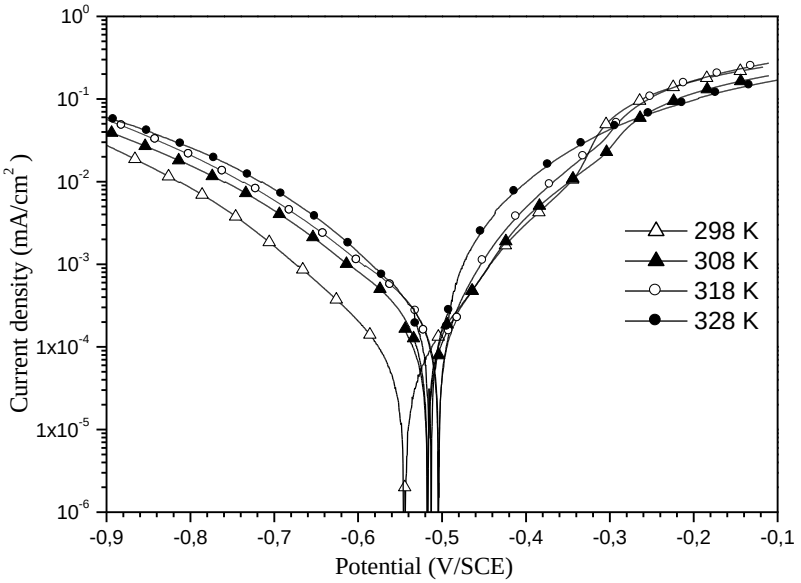

Fig. 9. Potentiodynamic polarization curves of mild steel in 1.0 M HCl at various concentration of **Q-Cl**

3.4. Effect of temperature

Temperature can modify the interaction between the steel electrode and the acidic media without and with substituted quinoline compounds inhibitor's. Polarization curves for mild steel in 1.0 M HCl in the absence and presence of 10^{-3} M of quinoline inhibitor's in the temperature range 298 K to 328 K are shown in Figures 7 to 9 presented the obtained potentiodynamic polarization curves and their corresponding data are presented in Table 7.

Table 7. Electrochemical and activation parameters and the corresponding inhibition efficiencies of mild steel in 1.0 M HCl at various temperature in absence and presence of 10^{-3} M of inhibitors

Inhibitor	Electrochemical parameters					Activation parameters		
	T (K)	E_{corr} (mV/SCE)	β_c ($mVdec^{-1}$)	i_{corr} (μAcm^{-2})	η_{pp} (%)	E_a ($KJ\ mol^{-1}$)	ΔH_a ($KJ\ mol^{-1}$)	ΔS_a ($J\ mol^{-1}K^{-1}$)
Blank	298±2	-485.0	-220.0	983	—	20.7	19.1	-129.6
	308±2	-450.0	-184.0	1200	—	—	—	—
	318±2	-453.0	-171.0	1450	—	—	—	—
	328±2	-447.0	-161.0	2200	—	—	—	—
Q-H	298±2	-545.3	-104.3	132	86.57	37.8	35.2	-90.3
	308±2	-552.3	-107.2	211	83.42	—	—	—
	318±2	-570.6	-109.8	300	79.31	—	—	—
	328±2	-527.8	-144.3	542	75.36	—	—	—
Q-Cl	298±2	-543.7	-90.1	96	90.23	42.5	40.4	-75.6
	308±2	-516.7	-127.1	183	84.75	—	—	—
	318±2	-503.5	-128.3	250	82.76	—	—	—
	328±2	-512.0	-130.1	455	79.32	—	—	—

The analysis of the results of Table 6, shows that density of the corrosion current gradually as the temperature increases and that, in the absence and presence of the inhibitors **Q-H** and **Q-Cl** Figures (8-10). The results show that the inhibitory effectiveness decreases

with increasing temperature, and the inhibitory efficacy of the compound **Q-Cl** to 10^{-3} M decreases to 79% at 328 K. The compound **Q-Cl** was found to be the best inhibitor for concentrations ranging from 10^{-3} to 10^{-6} M.

These results show that at high temperatures, these inhibitors do not have a pronounced inhibitory effect; therefore a use of these compounds in acidic solutions at elevated temperatures is not economical.

3.5. Kinetic parameters of activation

The influence of temperature on the inhibition process of metal corrosion by an inhibitor is an important tool through which insight into the performance of inhibitor, activation processes, and the nature of adsorption of inhibitor on the corroding metal surface can be gained. Based on the effect of temperature, Rodovici [33] grouped inhibitors into three categories: (i) those whose inhibition efficiency decreases with increase in temperature. In this category, the apparent activation energy E_a in the inhibited solution is higher than that in the uninhibited solution; (ii) inhibitors whose inhibition efficiency is unaltered with variation in temperature. Here, the E_a in the inhibited and uninhibited solutions does not change with rise in temperature; (iii) those whose inhibition efficiency increases with increase in temperature. In this class, E_a for the inhibited system is lower than E_a of the uninhibited system. The apparent activation energy, E_a of the corrosion reaction was determined using Arrhenius plots. The Arrhenius equation could be written as:

$$i_{corr} = A\exp\left(\frac{-E_a}{RT}\right) \quad (10)$$

Where i_{corr} is the corrosion current density, E_a is the apparent activation energy of the corrosion reaction and A is the Arrhenius pre-exponential factor.

The apparent activation energy of the corrosion reaction in presence and absence of the inhibitor could be determined by plotting *Ln* (i_{corr}) with *1000/T* which gives a straight line (Figure 10) with a slope permitting the determination of E_a. Figure 10 shows the Arrhenius plots in absence and presence of 10^{-3} M of quinoline inhibitor's. The corresponding values of E_a are given in Table 6 and indicate that values of E_a obtained in solutions containing **Q-Cl** and **Q-H** are higher than those in the inhibitor-free acid solutions. The higher values of the apparent activation energy obtained in the presence of these compounds compared with those obtained in its absence, coupled with the observed decrease in inhibition efficiency with rise in temperature suggest that some of **Q-Cl** and **Q-H** could be physisorbed on the steel surface [34].

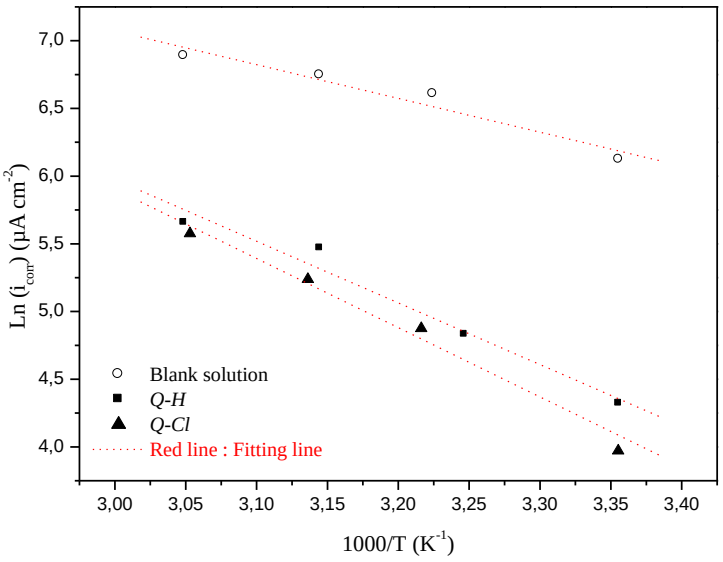

Fig. 10. Arrhenius plots of mild steel in absence and presence of optimum concentration of inhibitors **Q-H** and **Q-Cl**

An alternative formulation of Arrhenius equation (Eyring transition state equation) is [35]:

$$i_{corr} = \frac{RT}{Nh}\exp\left(\frac{\Delta S_a}{R}\right)\exp\left(\frac{\Delta H_a}{RT}\right) \qquad (11)$$

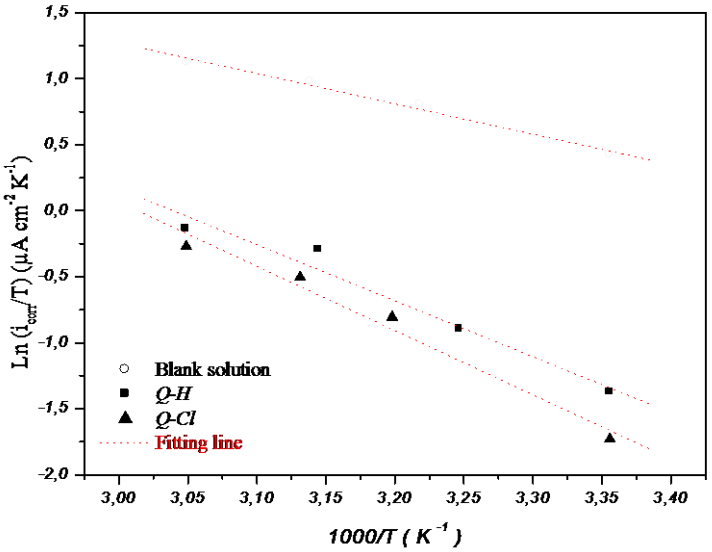

Fig. 11. Transition-state plots for carbon steel in 1.0 M HCl without and with 10^{-3} M of inhibitors **Q-H** and **Q-Cl**

Where *h* is Planck's constant, *N* is Avogadro's number, ΔS_a is the entropy of activation and ΔH_a is the enthalpy of activation. Figure 12 shows the variation of Ln(i_{corr}/T) function

(*1/T*) as a straight line with as lope of (*-ΔH$_a$/R*) and the intersection with the y-axis is [*Ln(R/Nh)* + (*ΔS$_a$/R*)].

From these relationships, values of *ΔS$_a$* and *ΔH$_a$* can be determined. The activation parameters *ΔH$_a$* and *ΔS$_a$* which determined from the slopes of Arrhenius lines without and with inhibitors are summarized in Table 7. It is seen that the *ΔH$_a$* value for dissolution reaction of mild steel in 1.0 M HCl in the presence of **Q-Cl** is higher than that in the presence **Q-H** and the free solution. In addition, the *ΔH$_a$* values in the presence **Q-Cl** and **Q-H** are higher than that in their absence. However, the positive signs of *ΔH$_a$* values reveal the endothermic nature of the mild steel dissolution process suggesting that is difficult with inhibitors.

Entropy of activation provides some further insight into the mild steel adsorption process. This parameter assists with information regarding the extent of disorder of the adsorption/desorption process between mild steel and inhibitor compounds. On comparing the values of entropy of activation *ΔS$_a$* listed in Table 7, it is clear that entropy of activation increases in the presence of the studied inhibitors compared to free acid solution. Such variation is associated with the phenomenon of ordering and disordering of inhibitor molecules on the mild steel surface. The increased entropy of activation in the presence of inhibitor indicates that disorderness is increased on going from reactant to activated complex. The increase in values of entropy by the adsorption of inhibitor molecules on metal surface from the acid solution can be regarded as quasi-substitution between the inhibitor molecules in the aqueous phase and H_2O molecules on electrode surface. In such condition, the adsorption of inhibitor molecules is followed by desorption of H_2O molecules from the electrode surface. Thus increase in entropy of activation is attributed to solvent (H_2O) entropy.

3.6. Isotherm and thermodynamic parameters of adsorption

Adsorption isotherms can provide basic information about the nature of the interaction between the inhibitor and the surface of the studied metal. However, in order to trace an isotherm, inhibition rates should be determined. On the other hand, the adsorption isotherm, which describes the adsorption behavior of organic inhibitors, is to know the corrosion inhibition mechanism between the inhibitor molecules and the metal surface. Several isotherms of adsorption have been studied to adjust the values of the degree of the covering surface according to the Langmuir isotherm [36-40], which is given by the following relationships (13,14). The constant of adsorption K_{ads} is related to the standard free energy of adsorption ΔG°_{ads}, with the following equation (10,11):

$$K_{ads} = \frac{1}{55.5}\exp\left(\frac{-\Delta G^{\circ}_{ads}}{RT}\right) \quad (13)$$

$$\frac{C_{inh}}{\theta} = \frac{1}{K_{ads}} + C_{inh} \quad (11) \qquad (14)$$

Where R is the universal gas constant, T the thermodynamic temperature, C_{inh} is the inhibitor's concentration, K_{ads} is the equilibrium constant for the adsorption-desorption process and the concentration of water in the solution is 55.5 mol/L.

A straight line was observed by plotting a graph between C_{inh}/θ *vs.* C_{inh} as shown in Figure 12, which suggested the adsorption of inhibitor molecules on the metal surface obeys Langmuir adsorption isotherm. The calculated values of ΔG°_{ads} and K_{ads} are given in Table 8.

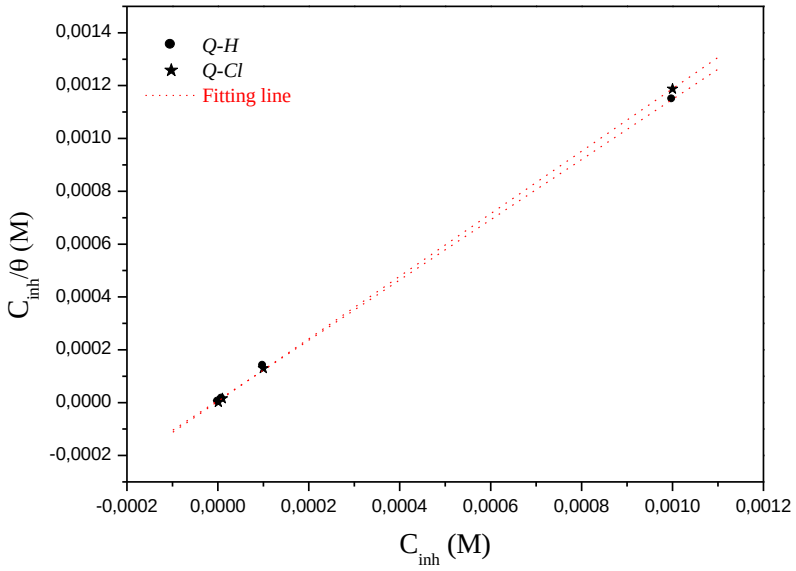

Fig. 12. Plot of the Langmuir adsorption isotherm of **Q-Cl** and **Q-H** on the mild steel surface at 298 K

Table 8. Value of constant K_{ads} and the free enthalpy calculated for the inhibitors from the Langmuir isotherm

Inhibitor	K_{ads} ***(L mol^{-1})***	R^2	ΔG°_{ads} ***(KJ mol^{-1})***
Q-Cl	407700.65	0.99999	-41.97
Q-H	268413.14	0.99998	-40.92

The C_{inh}/θ variation as a function of C_{inh} yields a straight line with a slope close to 1 and the linear association coefficient (R^2) is also nearly 1, indicating that the three inhibitors are adsorbed on the mild steel surface according to the Langmuir adsorption isotherm model [41].

Furthermore, it is recognized that the $-\Delta G^{\circ}_{ads}$ values of less than or equal to 20 KJ/mol indicate that the adsorption mode is physical, whereas those with values greater than 40 KJ/mol involve sharing or transfer of electrons from the inhibitor compound to the metal surface to form a co-ordinate type of bond (chemisorption) according to several authors [42-46].

In our case, the values of the free enthalpy of adsorption ΔG°_{ads} are greater than 40 KJ/mol for the three inhibitors. So, we can consider that these inhibitors are chemically adsorbed on the mild steel surface in 1.0 M of hydrochloric acid solution.

3.7. Scanning Electron Microscopy (SEM)

In order to evaluate the morphology of the surface of the steel to prove whether the inhibition is due to the formation of a film of organic molecules on its surface, we have used Scanning Electron Microscopy (SEM).

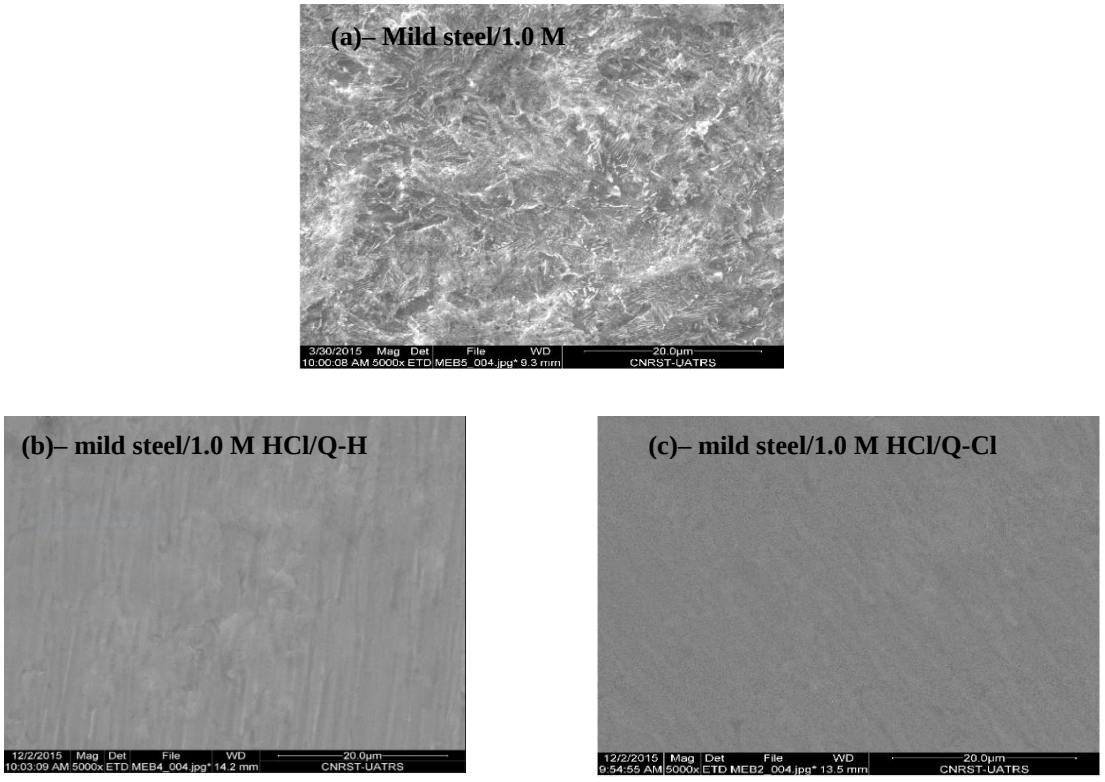

Fig. 14. Surface morphology of mild steel after immersion for 6 h in 1.0 M HCl (a) without inhibitors, (b) with 10^{-3} M of **Q-H** and (c) with 10^{-3} M of **Q-Cl**

The SEM micrograph of the deteriorated specimen after 24 h of immersion in 1.0 M HCl solution at 298 K is shown in Figure 14a. The image shows clearly that in the absence of the inhibitor, the surface of mild steel displayed a very irregular topography due to corrosion

attack. On the other hand, in the presence of the inhibitors **Q-H** and **Q-Cl**, We observe on the images of the steel surface after 24 h immersion in 1.0 M HCl medium at 298 K in the presence of 10^{-3} Mof **Q-H** and **Q-Cl** (Figures 14b and 14c) respectively. On the basis of these figures, it is obvious, that the surface is covered with a product in the form of a plate indicating the presence of an organic product. This observation shows that the inhibition is due to the formation of an adherent, stable and insoluble deposit, which limits the access of the electrolyte to the surface of the steel.

4. CONCLUSION

From the experimental results mentioned above, it can be concluded that:

- The studied compounds Q-H and Q-Cl exhibits good performance as inhibitors for mild steel corrosion in 1.0 M HCl solution, particularly at decreased temperature and increased inhibitor concentration.
- The polarization curves show that these compounds act as cathodic-type inhibitors. The adsorption of these inhibitors on the steel surface of 1.0 M HCl solution, follow the adsorption isotherm of Langmuir. The thermodynamic parameters indicate that this inhibitor is strongly adsorbed on the mild steel surface.
- The differences obtained between the results of gravimetric and electrochemical studies, related to the time of immersion of the steel in acidic medium.
- The results of Scanning Electron Microscopy analysis showed that, the mild steel surface was protected in the presence of both compounds.

REFERENCES

[1] Y. El Kacimi, R. Touir, M. Galai, R. A. Belakhmima, A. Zarrouk, K. Alaoui, M. Harcharras, H. El Kafssaoui, and M. Ebn Touhami, J. Mater. Environ. Sci. 7 (2016) 371.

[2] M. HazwanHussin, M. Jain Kassim, N. N. Razali, N. H. Dahon, and D. Nasshorudin, Arab. J. Chem. (2011) 1878.

[3] Y. El Kacimi, M. Achnin, Y. Aouine, M. Ebn Touhami, A. Alami, R. Touir, M. Sfaira, D. Chebabe, A. Elachqar, and B. Hammouti, Port. Electrochim. Acta 30 (2012) 53.

[4] E. A. Noor, and A. H. Al-Moubaraki, Int. J. Electrochem. Sci. 3 (2008) 806.

[5] M. El Bakri, R. Touir, M. Ebn Touhami, A. Srhiri, and M. Benmessaoud, Corros. Sci. 50 (2008) 1538.

[6] W. Li, Q. He, C. Pei, and B. Hou, Electrochim. Acta 52 (2007) 6386.

[7] Y. El Kacimi, M. A. Azaroual, R. Touir, M. Galai, K. Alaoui, M. Sfaira, M. Ebn Touhami, and S. Kaya, Euro-Mediterr. J. Environ. Integr. 2 (2017) 1.

[8] M. Scendo, and M. Hepel, Corros. Sci. 49 (2007) 3381.

[9] M. Galai, M. Rbaa, Y. El Kacimi, M. Ouakki, N. Dkhirech, R. Touir, B. Lakhrissi, and M. Ebn Touhami, Anal. Bioanal. Electrochem. 9 (2017) 80.
[10] A. Tazouti, M. Galai, R. Touir, M. Ebn Touhami, A. Zarrouk, Y. Ramli, M. Saraçoğlu, S. Kaya, F. Kandemirli, and C. Kaya, J. Mol. Liq. 221 (2016) 815.
[11] M. El Faydy, M. Galai, A. El Assyry, A. Tazouti, R. Touir, B. Lakhrissi, M. Ebn Touhami, and A. Zarrouk, J. Mol. Liq. 219 (2016) 396.
[12] M. Rbaa, M. Galai, M. EL Faydy, Y. El Kacimi, M. Ebn Touhami, A. Zarrouk, and B. Lakhrissi, J. Mater. Environ. Sci. 8 (2017) 3529.
[13] L. Tang, X. Li, Y. Si, G. Mu, and G. Liu, Mater. chem. Phys. 95 (2006) 29.
[14] M. S. Abdel-Aal, and M. S. Morad, British Corros. J. 36 (2001) 253.
[15] M. El Faydy, M. Galai, R. Touir, A. El Assyry, M. Ebn Touhami, B. Benali, and A. Zarrouk, J. Mater. Environ. Sci. 7 (2016) 1406.
[16] R. Karaman, and H. Hallak, Chem. Boil. drug design 76 (2010) 350.
[17] M. El Faydy, N. Dahaief, M. Rbaa, K. Ounine, and B. Lakhrissi, J. Mater. Environ. Sci. 7 (2016) 356.
[18] Y. Xia, Z. Y. Yang, P. Xia, K. F. Bastow, Y. Tachibana, S. C. Kuo, and K. H. Lee, J. Med. Chem. 41 (1998) 1155.
[19] Y. L. Chen, I. L. Chen, C. C. Tzeng, and T. C. Wang, Helv. Chim. Acta 83 (2000) 989.
[20] M. El Bakri, R. Touir, A. Tazouti, N. Dkhireche, M. Ebn Touhami, A. Rochdi, and A. Zarrouk, Arab J. Sci. Eng. 41 (2016) 75.
[21] L. Feng, X. Wang, and Z. Chen, Mol. Biomol. Spect. 71 (2008) 312.
[22] B. Fortenberry, B. Nammalwar, and R. A. Bunce, Org. Prep. Proced. Int. 45 (2013) 57.
[23] ASTM G-81., Annual Book of ASTM Standards, (1995).
[24] M. H. Wahdan, Mater. Chem. Phys. 49 (1997) 135.
[25] M. Stern, and A. L. Geary, J. Electrochem. Soc. 104 (1957) 56.
[26] Jr. O. L. Riggs, Corrosion Inhibition, second ed., C. C. Nathan, Houston, TX (1973).
[27] S. Ghareba, and S. Omanovic, Corros. Sci. 52 (2010) 2104.
[28] H. Gerengi, K. Darowicki, G. Bereket, and P. Slepski, Corros. Sci. 51 (2009) 2573.
[29] K. R. Trethewey, and J. Chamberlain, Corrosion for Science and Engineering. 2nd Edition, Edinburgh Gate Harlow, Essex CM20 2JE, England (1995).
[30] M. Behpour, S. M. Ghoreishi, N. Soltani, M. Salavati-Niasari, M. Hamadanian, and A. Gandom, Corros. Sci. 50 (2008) 2172.
[31] R. Solmaz, Corros. Sci. 52 (2010) 3321.
[32] M. Outirite, M. Lagrenée, M. Lebrini, M. Traisnel, C. Jama, H. Vezin, and F. Bentiss, Electrochim. Acta 55 (2010) 1670.
[33] O. Radovici, Proceedings of the 2nd European Symposium on Corrosion Inhibition Ferrara, (1965) 178.

[34] A. Benabida, M. Galai, M. Cherkaoui, and O. Dagdag, Anal. Bioanal. Electrochem. 8 (2016) 962.
[35] M. Behpour, S. M. Ghoreishi, N. Mohammadi, N. Soltani, and M. Salavati-Niasari, Corros. Sci. 52 (2010) 4046.
[36] A. O. Yüce, and G. Kardaş, Corros. Sci. 58 (2012) 86.
[37] D. Daoud, T. Douadi, and S. Issaadi, Corros. Sci. 79 (2014) 50.
[38] M. Lebrini, F. Robert, and H. Vezin, Corros. Sci. 52 (2010) 3367.
[39] R. Yıldız, T. Doğan, and I. Dehri, Corros. Sci. 85 (2014) 215.
[40] A. El Ouafi, B. Hammouti, and H. Oudda, In Annales de Chimie Science des Matériaux. 27 (2002) 27.
[41] K. Adardour, R. Touir, and R. A. Belakhmima, Res. Chem. Intermed. 39 (2013) 1843.
[42] Y. Abboud, A. Abourriche, and T. Saffaj, Mater. Chem. Phys. 105 (2007) 1.
[43] K. Alaoui, Y. El Kacimi, M. Galai, R. Touir, K. Dahmani, A. Harfi, and M. Ebn Touhami, J. Mater. Environ. Sci. 7 (2016) 2389.
[44] K. Alaoui, Y. El Kacimi, M. Galai, K. Dahmani, R. Touir, A. El Harfi, and M. Ebn Touhami, Anal. Bioanal. Electrochem. 8 (2016) 830.
[45] M. Galai, M. El Gouri, O. Dagdag, Y. El Kacimi, A. Elharfi, and M. Ebn Touhami, J. Mater. Environ. Sci. 7 (5) (2016) 1562.
[46] M. Benabdellah, R. Touzani, and A. Aouniti, Phys. Chem. News. 37 (2007) 63.

Copyright © 2017 by CEE (Center of Excellence in Electrochemistry)

ANALYTICAL & BIOANALYTICAL ELECTROCHEMISTRY (http://www.abechem.com**)**

Reproduction is permitted for noncommercial purposes.